JOURNAL OF SPACECRAFT AND ROCKETS
Vol. 40, No. 4, July–August 2003

# Applying Jet Interaction Technology

Louis A. Cassel*
*Northrop Grumman Mission Systems, San Bernardino, California 92402*

**The state of the art in aerodynamics engineering associated with the design and/or evaluation of reaction controls on flight vehicles operating in the atmosphere is reviewed. Various configurations of the aerodynamics interference problem are described to partition domains of the problem. To maintain an applications frame of reference, those descriptions are in the context of the dominant phenomenology observed under differing flight environment and vehicle geometry combinations. Following that, approaches to predicting or evaluating interference effects are reviewed. Approaches to the design of subscale wind-tunnel tests are discussed with a view toward relating appropriate scaling law approximations to the different domains of dominant phenomenology. Then results, found in the literature, describing the evolution of analytical and computational modeling are reviewed. Finally, some conclusions and observations on the state of the art are offered.**

## Nomenclature

| | | |
|---|---|---|
| $A$ | = | reference area |
| $a$ | = | speed of sound |
| $C$ | = | coefficient of specific heat |
| $C_D$ | = | drag coefficient |
| $C_T$ | = | thrust coefficient |
| $c$ | = | discharge coefficient of jet nozzle |
| $d$ | = | diameter of jet nozzle (throat unless otherwise specified) |
| $E$ | = | energy |
| $h$ | = | measure of jet plume height |
| $K$ | = | amplification factor defined in Eq. (2); species concentration |
| $k$ | = | coefficient of thermal conductivity |
| $l$ | = | control moment lever arm |
| $M$ | = | Mach number, $V/a$; control moment |
| $m$ | = | mass; mass flow rate when dotted; molecular weight when scripted |
| $P$ | = | pressure |
| $Pr$ | = | Prandtl number; Eq. (4) |
| $q$ | = | dynamic pressure |
| $R$ | = | gas constant |
| $Re$ | = | Reynolds number; Eq. (4) |
| $T$ | = | jet thrust; temperature |
| $V$ | = | velocity |
| $v$ | = | vacuum conditions; flight vehicle parameter |
| $x, y, z$ | = | conventional body-fixed axes coordinates |
| $\alpha$ | = | angle of attack |
| $\gamma$ | = | ratio of specific heats |
| $\mu$ | = | coefficient of viscosity |
| $\rho$ | = | density |

*Subscripts*

| | | |
|---|---|---|
| $e$ | = | flow condition at the edge of the mainstream flow boundary layer |
| $j$ | = | jet flow (at sonic point unless otherwise specified) |
| 0 | = | stagnation condition for flow parameter |
| 1 | = | flow condition in a uniform mainstream |
| $\infty$ | = | freestream flow condition outside the influence of the vehicle or jet |

Received 12 March 2003; revision received 12 March 2003; accepted for publication 8 May 2003. 

*Advanced Projects Manager, Missile Defense Division Western Operations. Member AIAA.

## I. Introduction

FOR more than 40 years it has been recognized that operation of reaction controls on vehicles in atmospheric flight results in aerodynamic interference between the reaction control plume and flow over the vehicle. The result of that interference is a change in the pressure distribution (and, in supersonic flight, the aeroheating distribution) on the vehicle surface. That is, qualitatively, the activation of the reaction control produces forces and moments on the vehicle that are similar to those resulting from the deployment or deflection of a control surface. These aerodynamics forces and moments add to the reaction thrust forces produced by the jet. It is a vector addition because the aerodynamic interference-induced forces can frequently be in different directions than that of the reaction control force.

A great deal of research, analytical and computational modeling, as well as ground and flight testing has been associated with these aerodynamics interference effects. Applications have been mostly in connection with missiles and reentry vehicles. Several surveys have reviewed various aspects of research and engineering addressing the phenomena. In the early stages of the development of understanding and applications, Spaid and Cassel surveyed the understanding of the phenomenology and applications in the unclassified literature in 1973, as reported in Ref. 1. That survey relates references, in a bibliography of 93 citations, to aspects of the phenomenology to which they pertain. Recently, Roger surveyed the applications literature in Ref. 2. A bibliography of 169 references that document applications, wind-tunnel and flight testing over the past 40 years, many of them previously classified, is provided in that survey. It summarizes aspects of the interaction phenomena and parameters for scaling wind-tunnel testing for control system design applications.

The objectives of this review are 1) to summarize the state of the art in understanding the phenomena that occur with respect to reaction control operation on missiles and reentry vehicles, 2) to review the considerations and theories associated with the design of subscale wind-tunnel testing to simulate the phenomena, and 3) to review the progress in analytical and computational modeling of the interference effects induced by the phenomena.

In this survey, various configurations of the aerodynamics interference problem are described to partition domains of the problem. To maintain an applications frame of reference, those descriptions are in the context of the dominant phenomenology observed under differing flight environment and vehicle geometry combinations. Following that, approaches to predicting or evaluating interference effects are reviewed. Approaches to the design of subscale wind-tunnel tests are discussed with a view toward relating appropriate scaling law approximations to the different domains of dominant phenomenology. Then results, found in the literature, describing the evolution of analytical and computational modeling approaches are reviewed. Finally, some conclusions and observations on the state of the art are offered.

## II. Domains of the Problem

The phenomena defining the domain of this review are the interactions of the plume from a sonic or supersonic reaction control nozzle with a transverse flow engulfing the plume. In some configurations there are multiple nozzles and plumes. This defining phenomenon is common to all configurations of reaction control induced aerodynamic interference considered. As shown in Fig. 1, the plume is turned by the transverse flow, and the transverse flow is diverted by the presence of the plume. The transverse flow boundary layer over the vehicle surface is separated upstream of the nozzle exit. A wake is created on the leeside of the plume relative to the transverse flow. Vortices are formed in this wake. Which of these phenomena dominate depends on the flight conditions, the plume conditions, the geometry of the vehicle, and the location of the plume relative to that geometry.

In general, discussions in this review will address the interactions of a non-reacting perfect gas jet with flow in a perfect gas atmosphere. The two perfect gases are presumed to have different properties. This is the problem studied in most experimental and computational investigations reported in the literature. There are two considerations that may have major effects on all of the phenomena involved. These are the location and behavior of boundary-layer transition on the flight vehicle and the presence of chemistry in the nozzle plume (or in the transverse flow under some hypersonic flight conditions). These are not addressed in the following discussion of phenomena domains, scaling, or prediction methods. They are discussed later in separate sections. As described there, there are particular situations where these aspects of the flow are dominating considerations. Boundary-layer transition can dominate the interaction phenomenology behavior in two-dimensional flows. Reactions can have a significant effect on control forces in circumstances where the jet plume chemistry includes significant combustion in the plume interaction region.

As in most aerodynamics problems, the most fundamental change in governing phenomena is the presence, or absence, of shock waves

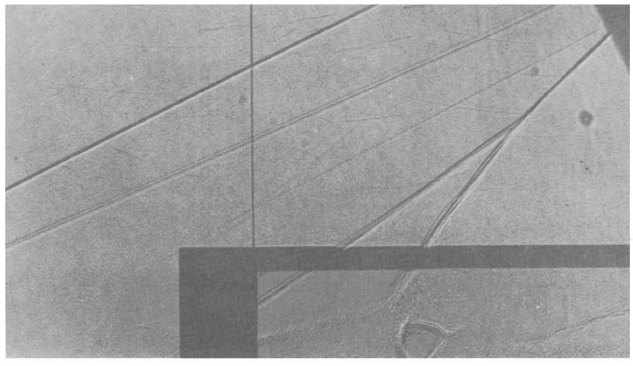

a) Shadowgraph photograph of typical jet interaction flowfield, turbulent boundary layer, $M_1 = 2.61$

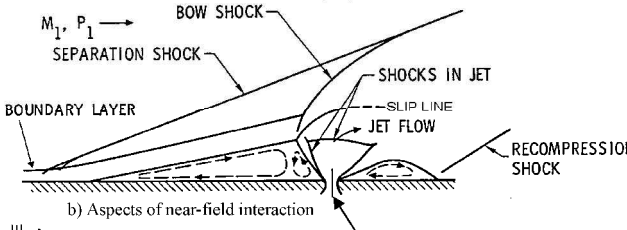


b) Aspects of near-field interaction

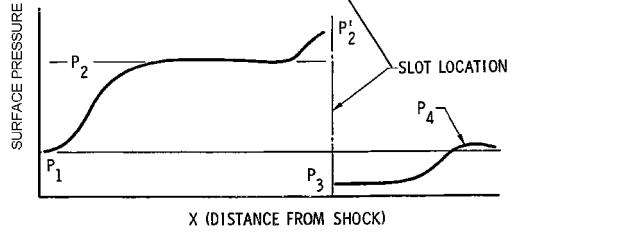


c) Typical interaction pressure ($P_x$) distribution

**Fig. 1 Interaction region centerline plane.**

(other than those in the jet plume) in the interaction region. Consequently, interaction phenomena in supersonic flight behave differently than those in subsonic flight. The emphasis here, as it has been in applications, is on the supersonic flight case. However, the differing behavior of interactions in subsonic flight will be summarized.

### A. Near-Field Interactions

Most of the literature addressing reaction control-induced interactions deals with the phenomena in the immediate vicinity of the jet exit. In designing for favorable interference, it is the magnitude and distribution of interaction-induced pressures on the vehicle surface in this region that provide the favorable amplification of reaction control forces.

#### *1. Interaction in Supersonic Flight*

When the flight Mach number is supersonic, the phenomena in the interaction region near the jet plume can be viewed as the superposition of three-dimensional effects on an idealized, two-dimensional interaction. In the idealized case, the flow over the vehicle surface is presumed to be uniform and parallel. The jet exit is an infinite span slot aligned perpendicular to the flow. A schlieren photograph of a wind-tunnel representation of such a flow is shown in Fig. 1.

The vehicle model in this hypothetical case is a two-dimensional planer wing with a sharp leading edge. Qualitatively, the resulting interaction flowfield is representative of the plane of symmetry of a three-dimensional interaction with a plane of symmetry. An example of the latter is the interaction in the plane of symmetry of a body of revolution, for example, cone or ogive-cylinder, with a circular nozzle jet aligned in that plane. A more complex example is an aircraftlike configuration with a similarly aligned circular jet nozzle. The analogy holds even when angle of attack is introduced, as long as the geometry and flow have a common plane of symmetry. (Differences between the two-dimensional flow and the flow outside the plane of symmetry of the three-dimensional flow will be discussed later.) The major features of the two-dimensional flow are illustrated in Fig. 1 from Ref. 1. Detailed descriptions are found in Refs. 3–5.

The shock structure within the underexpanded jet that interacts with an external flow is quite similar to the shock structure within an underexpanded jet exhausting into a quiescent medium for at least a few exit diameters from the exit plane. When the jet is highly underexpanded, most of the jet flow passes through a normal shock before it is turned to the external-flow direction. A shear layer surrounds the jet plume at the exit.

In the flowfield shown in Fig. 1, the boundary layer is separated upstream of the jet location and a shock wave, labeled separation shock, originates near the separation line. The separated external-flow boundary layer meets the shear layer at the upstream boundary of the jet to form the mixing layer between the jet plume and the external flow. A shock wave, labeled bow shock in Fig. 1, originates in this region. The multiple images that can be seen for the separation shock, the bow shock, and the recompression shock indicate that the flow is somewhat unsteady and that the distance through which the shock waves move is much smaller than the separation distance. Studies of supersonic and hypersonic turbulent boundary-layer flow over solid spoilers and ramps, including measurements of static pressure fluctuations, such as those in Refs. 6 and 7, have shown a significant degree of flow unsteadiness in the separated region. The static pressure $P_1$ rises in the vicinity of separation, reaches a plateau, $P_2$ (data from some experiments show a first peak), and rises again in the immediate vicinity of the jet, $P_2'$. Static pressure and flow-visualization data indicate that this pressure distribution is the same whether the flow interference is caused by a jet or by a forward-facing step. However, to satisfy the boundary conditions, when a jet causes the separation, at least two counter-rotating vortices are required within the upstream separated region.

A second separated region exists downstream of the jet. This region has some of the characteristics of the separated region found in flow over a rearward-facing step. When the external flow is supersonic, the static pressure immediately downstream of the jet, $P_3$, is less than the static pressure of the undisturbed flow, $P_1$ as

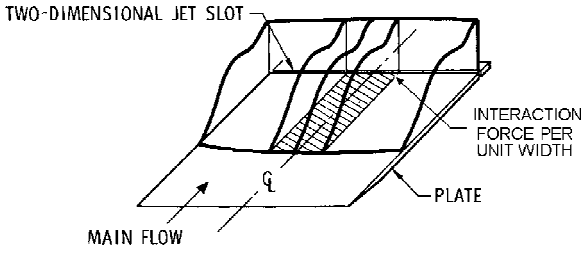


**a) Two-dimensional interaction**

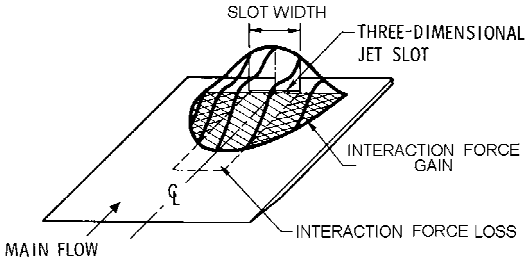


**b) Three-dimensional interaction**

**Fig. 2 Effects of finite span nozzles in uniform flow.**

shown in Fig. 1. The geometry of the downstream separated region shown in Fig. 1 implies a wake followed by a component of velocity normal to the wall upstream of reattachment. A recompression shock is required to turn the flow parallel to the wall. In hypersonic flow, downstream pressure distributions in which the ratio $P_4/P_1$ is always greater than unity are reported in several sources, such as Ref. 8.

The most prominent three-dimensional effects, away from the plane of symmetry in the vicinity of the jet exit, are those due to the wraparound of the interaction bow shock. These are most easily visualized by replacing the infinite span slot jet in the hypothetical interaction model with a finite width slot (or circular cross section) jet nozzle. Figure 2 (following Ref. 9) shows static pressure distributions for nearly two-dimensional flow and for a finite-span slot. In the case of the finite-span slot, the length of the separated region decreases, and the interaction region extends outboard from the ends of the slot. If the height of the effective obstruction produced by the jet is sufficiently small relative to the slot span, the plateau pressure measured along the centerline plane of symmetry will remain almost unchanged.

The principal difference between phenomena in the idealized situation (representing an infinite span jet) and the situation where the plume span is finite is the downstream running parabolic locus of the interaction region around the jet plume. In contrast to the two-dimensional situation, in which the entire external flow must go over the jet-induced obstruction, the flow can go around the three-dimensional jet, resulting in a curved interaction shock. As shown in Fig. 2, this difference changes both the shape and the extent of the interaction region. In the centerline plane of symmetry, the length of the interaction region is shortened, reducing the interaction forces. At the same time, higher pressures near the interaction shocks are wrapped around the plume, adding to the interaction force component generated in this region. Whether the net effect is an addition or subtraction, for a finite-span plate, is likely to depend on all of the parameters that effect the interaction. From an applications perspective, it is more important to consider the complexities introduced, in the three-dimensional case, by vehicle geometry differing from the idealized flat plate.

When the flat plate geometry is replaced with a body of revolution, the fundamental near-field phenomena present in most applications of reaction controls to flight vehicles can be visualized. An example is the interaction between an axisymmetric underexpanded jet and flow over an axisymmetric (ogive-cylinder planform) surface from which the jet exhausts. This phenomenon is shown in Fig. 3. The shadowgraph photograph and photograph of an oil-flow experiment are from data reported in Ref. 10. The jet exhausts from a sonic orifice located on the midbody of an ogive-cylinder at zero

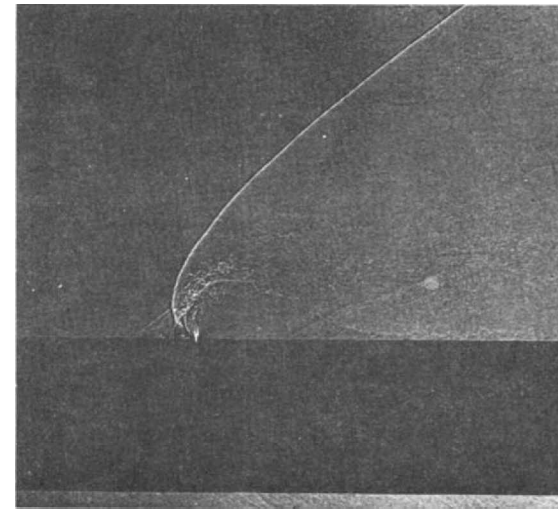

**a) Shadowgraph of interaction region**

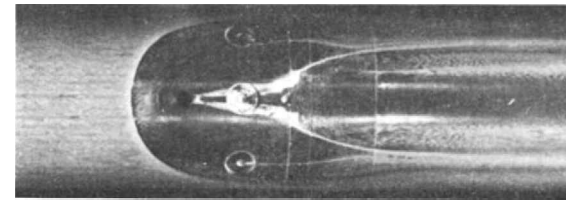

**b) Oil flow on the surface of interaction region**

**Fig. 3 Jet interaction on an ogive-cylinder body of revolution.**

angle of attack. The boundary layer approaching the jet is turbulent. Interpretations of this flow have been offered in Ref. 11.

As shown in Fig. 3a, the jet plume presents an obstacle to the external flow, which causes a strong shock and separates the boundary layer upstream of the jet, just as in the case of the flat plate. As a result of high pressures immediately downstream of the plume induced boundary-layer separation, and mixing between the two streams, the jet is turned in the direction of the external flow. A three-dimensional shock structure forms in the jet plume as it is turned, bounded by a three-dimensional mixing layer. Strong mixing is indicated by the turbulence near the leading edge of the jet plume. The mixing layer surrounds the plume and reattaches to the body downstream (approximately one body diameter downstream of the jet exit in Fig. 3). Downstream of the jet exit, in the region where the mixing layer surrounding the jet reattaches to the body, a set of vortices forms in the jet wake. The patterns in the oil flow, on the sides of the jet wake, shown in Fig. 3, are believed to be related to these vortices. A wide range of flow-visualization data for jet-induced interference on bodies of revolution is provided in Ref. 10.

### 2. *Interaction in Subsonic Flight*

In the literature, and probably in application, far less attention has been given to the interaction of underexpanded jets with mainstream flows in subsonic flight. The principal occurrence of this situation has been with reaction-controlled tactical missiles. A broad evaluation of the jet interaction phenomena associated with this subsonic mainstream was given in Ref. 12. A comparison of interaction flows in supersonic and subsonic flight conditions is shown in Fig. 4. These shadowgraphs illustrate the dramatic differences in the apparent penetration of the jet into the mainstream in the two cases. As discussed in Ref. 12, the dominating scale factor for the subsonic flight case is the height of the strong shock (frequently called the Mach disk) in the underexpanded jet plume. (Recall the restriction of the domain of interest here to interference involving sonic and supersonic jet plumes, as opposed to interference involving subsonic jets that is included in Ref. 12.) In the absence of the pressure increase associated with the shock waves in supersonic flow, the jet plume is virtually undisturbed by the mainstream until after the dynamic pressure of the jet is reduced by the strong shocks in the plume.

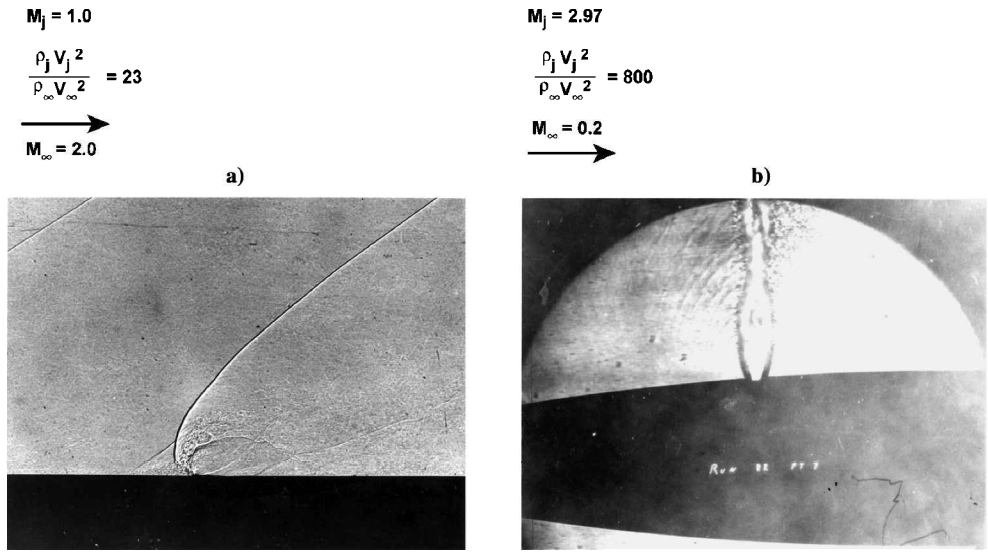


**Fig. 4 Interaction in supersonic and subsonic mainstreams, shadowgraphs of interaction flowfield (*U*) (data from D. J. Spring, AMICOM).**

As illustrated in Ref. 12, interference pressure distributions, in the region of the jet plume, are similar to those observed in supersonic flight for Mach numbers at least as low as 0.8. However, for very low freestream velocity, at least up to a Mach numbers of 0.2, the interference pressures behave much differently than those associated with supersonic flight. As discussed in Ref. 12, in connection with subsonic jets interacting with subsonic flows, a limiting interaction condition exists when the freestream velocity approaches zero. In the limiting case, the jet is the only significant flow, and only the jet affects the pressure distribution on the surface from which it exhausts. The result, for a circular nozzle, is a near axisymmetric interference pressure distribution. In this case, approximated by the flow illustrated in Fig. 4, the jet acts like a pump entraining the ambient air. The result is negative pressure coefficients throughout the interaction region.

As described in Ref. 12, the conventional interference pressure coefficient, normalized by freestream dynamic pressure, is singular in the limiting case of zero freestream velocity. To address this singular behavior, the analyses reported in Ref. 12 define an interference pressure coefficient normalized by ambient static pressure rather than dynamic pressure. It could be argued that the jet dynamic pressure is the more meaningful normalizing parameter in the limiting case. The logic for selecting the Mach number where transition occurs from one normalization to the other, irrespective of which normalizing criterion is chosen, is yet to be deduced for flight vehicle applications.

With use of data from Ref. 13, interference pressures induced by plumes from rectangular slot nozzles are analyzed in Ref. 12. The data include slot nozzles of two different aspect ratios, on an ogive-cylinder body of revolution, with the jet axis perpendicular to the mainstream. The difference in behavior between interaction pressures associated with these and interaction pressures associated with circular nozzles is distinct. When the nozzle is rectangular, the interference pressures fail to correlate with dimensions associated with the size of the jet plume, even when the subsonic Mach number is high. Consequently, it is concluded that they are affected by some interaction phenomena other than blockage. Clearly the entrainment phenomenon that dominates the limiting case of vanishing mainstream velocity is always present. It is likely that this influence of viscous mixing at the jet boundary is enhanced by the distinctly different geometry of the boundary, particularly the relatively angular edges of the plume, in the case of rectangular slot nozzles. As discussed in connection with interactions between subsonic jets and subsonic streams in Ref. 12, it is likely that the mixing process at the jet boundary generates streamwise vortices. In supersonic mainstreams, these vortices do not appear to influence the interaction pressures until a distance downstream of the nozzle is reached, where the jet plume is turned to the streamwise direction.

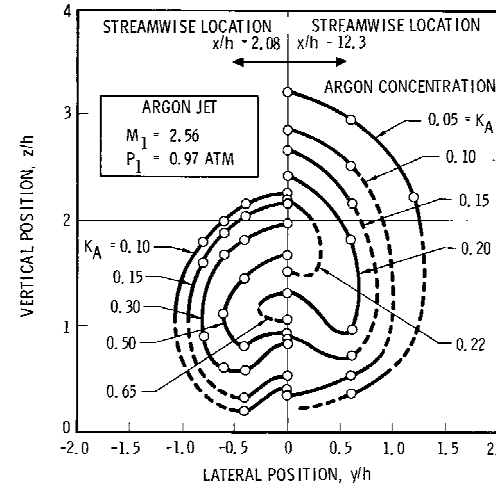


**Fig. 5 Jet concentration profiles in the interaction wake.**

In the case of slot nozzles in subsonic flow, they appear to influence interaction pressures in the vicinity of the jet exit.

### B. Far-Field Interactions

There is substantial evidence that, in supersonic flight conditions, the influence of the interaction persists far downstream of the jet plume (where that distance is measured in comparison to the penetration of the jet into the mainstream). Figure 5 shows cross sections of jet concentration contours from Ref. 14, as described in Ref. 1. These were measured at locations 2.08 and 12.3 times the penetration height downstream of a point where the forward extrapolated bow shock would intersect the surface forward of the jet exit. The penetration height is calculated from the momentum balance relationship in Eq. (1) from Ref. 15. This persistence is manifested in a wake of the interaction region that affects pressure distributions on surfaces of the flight vehicle far downstream of the jet exit. The effects can range from subtle mass and energy addition to the presence of an otherwise (jet off) separated flow region to very dynamic impingement on downstream surfaces by the plume:

$$\frac{h}{d} = \frac{1}{M_1}\sqrt{\frac{2P_{0j}\gamma_j}{C_P^* P_1 \gamma_1}}\left[\left(\frac{2}{\gamma_j - 1}\right)\right.$$

$$\left.\times\left(\frac{2}{\gamma_j + 1}\right)^{(\gamma_j+1)/(\gamma_j-1)}\left(1 - \frac{P_1}{P_{0j}}^{(\gamma_j-1)/\gamma_j}\right)\right]^{\frac{1}{4}} \qquad (1)$$

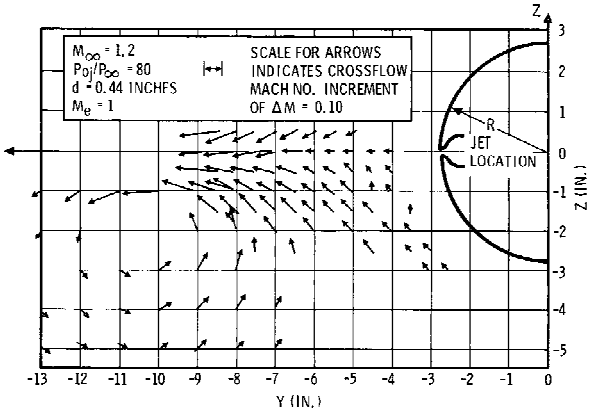


**Fig. 6 Vortices in the wake of the interaction region.**

One phenomenon associated with the downstream wake of the interaction can be quite significant in some practical applications. It has the potential to generate forces and moments on aerodynamic surfaces relatively far downstream of the jet nozzle exit. The wake includes a vortex field aligned generally in the direction of the mainstream flow. Because of this alignment, forces produced on downstream surfaces are likely to have components that are not aligned with the jet thrust. The result is usually the occurrence of aerodynamic moments out of the plane of the jet thrust vector (or cross coupling moments) induced by activation of the reaction controls.

The magnitudes of components of lateral velocity in the jet-induced vortices have been reported by Dahlke.[16] An example of measurements made by Dahlke is shown in Fig. 6. The velocities were measured with a calibrated multi-orifice pressure probe. They are in the cross section plane, 8.63 body diameters downstream of a sonic jet exit. The jet exit is three calibers from the origin of a four-caliber ogive nose. It exhausts normal to the surface of an ogive-cylinder at zero angle of attack. Durando and Cassel have derived correlations of data such as these to model the strength of these vortices.[12]

### C. Influence of Boundary-Layer Transition

Jet interaction is a shock–boundary-layer interaction phenomenon in supersonic flow, and it clearly involves viscous shear layer mixing and entrainment in subsonic flows. Consequently, the phenomena associated with it are influenced by the state of the boundary layer relative to transition from laminar to turbulent flow. When that state is near transitional, the interaction phenomena have been observed to influence the state, that is, propagation of the separated flow region described in Sec. II.A upstream can accelerate transition if the interaction is near the transition points.

Reference 1 documents the substantial research associated with relating the two-dimensional jet interaction upstream phenomena to the behavior of boundary-layer separation upstream of forward-facing steps. The interaction flowfield phenomena are clearly dominated by the condition of the boundary layer and are Reynolds number dependent when the boundary layer is laminar.

In the three-dimensional-flow case, when the plume span is small relative to dimensions of the vehicle in the vicinity of the interaction, the dependence of the interaction on the condition of the boundary layer approaching the interaction region is not well established. An important example illustrating this condition is a small-radius circular nozzle jet exhausting from a body of revolution, where the nozzle radius is small compared to the body radius. Unfortunately, it is not clear what geometry or flow conditions in the flow interaction affect the change, from dominance of the interaction by the transition condition of the boundary layer, to relative insensitivity to it.

In practice, the design engineer is well advised to pay close attention to the state of the boundary layer in any of the approaches to jet interaction engineering solutions discussed in Sec. III.

### D. Influence of Flow Chemistry

Since jet interaction phenomena involve two flows, there are aspects of flowfield chemistry associated with both of them, and in some cases with the relationship between them.

The chemistry in the mainstream flow is only a concern in high Mach number hypersonic flight. Obviously, the effects that influence the aerodynamics and aerothermodynamics of the vehicle in the absence of the jet apply to the jet interaction effects. In this flight condition, the jet interaction bow shock described in Sec. II.A is a very strong shock. On otherwise slender body vehicle configurations, it may generate temperatures, and therefore flow chemistry, not present elsewhere in the vehicle flowfield.

The flow chemistry associated with the jet plume has several facets, depending on the design of the interaction system. An approach to interaction enhancement in some applications is to deliberately formulate the reaction control propellants to create exothermic reactions in the plume interaction. This has been referred to as external burning jet interaction. There is a body of applications literature, including models for predicting the interaction enhancement summarized in Ref. 2. Even when this is not an aspect of the design, the possibility of afterburning in the plume is frequently present. The methods of analysis developed for external burning jet interaction should be considered if this phenomenon is expected to be significant. The potential for applications of computational methods is summarized in Sec. IV.B.

## III. Engineering Problems

The design of a reaction-control system for an environment where aerodynamic interference will occur adds substantial aerodynamics complexities to the conventional problem of designing reaction-control systems for operation in a vacuum. To differentiate the former, the control system will be referred to as a jet interaction (JI) control system in the following discussion. In the engineering applications involving JI-control systems, there are two classes of problems most commonly encountered. One class addresses the design of a JI-control system. Its solution is the configuration of jet and vehicle parameters, with the most efficient combination of reaction and aerodynamic interference forces that provides attitude control over the intended flight envelope. The other class addresses the evaluation of unintended aerodynamic interference forces on a configuration designed for an environment where aerodynamic interference is absent (or not anticipated). Its solution is the characterization of the variation of the interaction-induced forces with the parameters describing the flight envelope. In most cases of the former class encountered by the author, the designer selecting the vehicle/control configuration focuses on local, favorable interaction effects in the vicinity of the jet exit. In cases involving the latter class, the principal concern is usually with unfavorable interaction effects at locations on the vehicle more remote from the jet nozzle exit.

### A. Designing for Favorable Jet Interaction

The principal objective in the design of attitude control systems is to create and sustain attitude trim moments over a specified flight envelope. The optimization objective is to generate attitude control moments, about the vehicle c.g., with minimum weight and volume of apparatus and minimum expenditure of control actuation energy. For reaction-control systems, this generally leads to selection of the configuration requiring minimum thrust. The first design attribute sought is localization of the control force as far as possible from the c.g., thus, maximizing the control moment associated with any force produced. This attribute is attained when the center of the interference-induced forces is close to the reaction jet nozzle exit. For supersonic flight applications, there is a large base of experience providing guidance toward achieving these objectives. For subsonic flight applications, the description in Sec. II of pressures induced by interaction of a jet plume with a subsonic stream indicates that designing for favorable interaction forces is more problematic.

In some recent applications, another objective has been added to the reaction control implementation. As discussed in many of the references in Sec. IV.B, the reaction control on some ballistic missile defense interceptors is sized to provide maneuver forces under low dynamic pressure flight conditions. In these cases, the thrust magnitude must be of the order of the aerodynamic forces (or larger). Under these circumstances, the plume dimension will

be comparable to a body dimension. Both the low dynamic pressure and the large plume conditions drive the interaction phenomena to the region where the amplification factor will be low (or even negative).

It has become common to define the net control force produced by a JI control in terms of a parameter referred to as the amplification factor. In this discussion, two amplification factors are used. One is the force amplification factor $\boldsymbol{K}_F$. The other is the moment amplification factor $\boldsymbol{K}_M$. The force amplification factor is defined as the ratio of the total force produced, by the sum of the thrust and aerodynamic interference, to the thrust of the jet in a vacuum:

$$\boldsymbol{K}_F = (\text{thrust} + \text{interaction force})/\text{vacuum thrust} \tag{2}$$

where $\boldsymbol{K}_F$ is a vector and vacuum thrust is a scalar. It is important to separate the vector components of the amplification factor when there is no plane of symmetry in the flowfield.

The moment amplification factor is the ratio of the control moment produced to the moment (about a specified reference) that is produced by the vacuum thrust of the reaction control. In this definition, the vacuum thrust moment is a scaler. The moment amplification factor and the total control moment are considered to be vectors, that is,

$$\boldsymbol{K}_M = (\boldsymbol{M}_{\text{on}} - \boldsymbol{M}_{\text{off}})/|l T_v| \tag{2a}$$

where

$\boldsymbol{M}_{\text{on}}$ = moment about reference with jet on
$\boldsymbol{M}_{\text{off}}$ = moment about reference with jet off
$l$ = moment arm of thrust to reference
$T_v$ = vacuum thrust

The objective of JI-control system design is to realize high-amplification factors. Typical values of force amplification factors, achieved with circular nozzles on a flat plate, are shown in Fig. 7, from Ref. 1. As indicated by these data, it is quite common (in applications that lend themselves well to JI controls) to experience forces due to the aerodynamic interaction that are larger than the thrust force. In general, that is only the case when the size of the jet plume is small compared to the cross-sectional radius of curvature of the vehicle at the jet location. The size of the jet plume must be determined from a meaningful scaling parameter, such as determined by Eq. (1) or equations such as those discussed in Sec. IV.

### 1. *Influence of Jet Location on Vehicle*

The description in Sec. II of the interaction phenomena near the jet exit in a supersonic mainstream indicate an increase in pressure forward (upstream) of the jet exit. These (favorable) interaction pressures follow the locus of the JI bow shock intersection with the vehicle surface in near parabolic contours around the jet (in the absence of local vehicle geometry discontinuities) as shown in Figs. 2 and 3. Directly downstream of the jet exit are pressure reductions on the vehicle surface, in the wake of the flow around the plume, as shown in Fig. 1. It seems obvious then, and has indeed been shown to be the case, that the JI-control configuration approach is to locate the jet exit near the aft extent of the vehicle surface. This creates the largest control moment arm available while minimizing the vehicle surface area affected by the pressure reductions downstream of the jet exit.

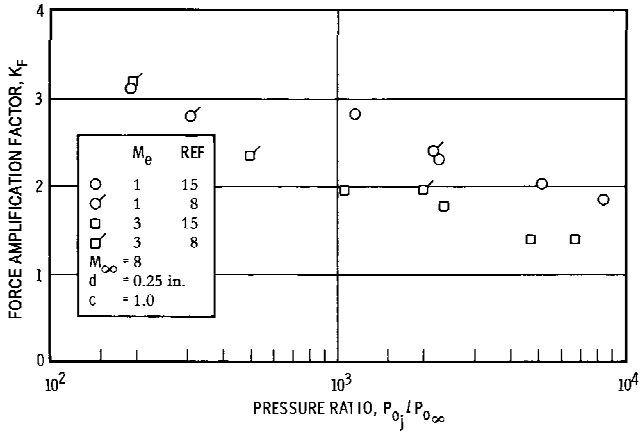


**Fig. 7 Typical force amplification factors on a flat plate.**

Conversely, locating the jet exit forward on the vehicle exposes lifting surfaces downstream of the plume interaction to the generally unfavorable interference phenomena in the wake of the principle interaction. These begin with the pressure reduction on the vehicle surface directly downstream of the jet exit, which results in a force component opposing the thrust direction. Whether this unfavorable effect counters the influence of pressure increase along the interference bow shock contour depends on the ratio of the interaction disturbance height to the local radius of curvature of the vehicle surface transverse to the flow. When the ratio is large, and the curvature is convex, the shock wraps around to surfaces where the force elements due to the interference pressure increase are either less effective in or counter the direction of the reaction thrust. As the relative disturbance size is reduced, more of the pressure increase contour is effective in generating favorable direction force elements. Finally, if the curvature is concave (or if the local interaction region is confined by elements of vehicle surface, such as fins or strakes, which confine the interaction shock) the interaction bow shock can be amplified by reflection. In this latter case, the favorable effects can definitely overcome the unfavorable effects of pressure reduction in the wake of the plume.

A typical result of locating the jet forward, on a continuously convex body of revolution, is shown in Fig. 8, from Ref. 11. These results represent an opposing extreme in comparison with the results for the aft-mounted jets, on an idealized configuration with no curvature in the crossplane, in Fig. 7. Obviously, the interaction can be so detrimental as to negate the control moment expected in the absence of interaction. As shown in the inset in Fig. 8, the configuration to which these data apply not only has the jet located forward, but also has lifting surfaces downstream of the jet. Consequently, they may interact with the jet wake. An example of this type of interaction is discussed in connection with JI on the space shuttle in Sec. III.B.

### 2. *Influence of Jet Nozzle Parameters*

As discussed in Ref. 1, a good deal of research has been dedicated to evaluation of the effect of jet exit Mach number on the interaction phenomena. In general, undergoing expansion in the nozzle, a supersonic jet expands less at the nozzle exit and presents a narrower obstruction to the external flow than an underexpanded sonic jet having the same mass flow rate. Therefore, higher exit Mach number jets cause relatively smaller interference forces when the nozzle is perpendicularto the mainstream flow. This effect is shown in Fig. 7. In this case, data are presented in the form of amplification factor vs pressure ratio for constant external flow conditions and constant nozzle throat diameter. Note that the decrease in interaction force resulting from the increase in $M_e$ is a larger effect than the increase in jet thrust. The effect of inclining the thrust axis of a circular jet relative to the external flow direction has been investigated in several experiments, such as those reported in Refs. 17 and 18. In general, inclining the nozzle upstream will increase the effective disturbance size and the interaction force. The penetration height model represented by Eq. (1) from Ref. 15 was modified in Ref. 17 to include the effects of forward inclination. The result is that at the penetration height $h$ given in Eq. (1) must be multiplied by the ratio

$$h/h_{\text{normal}} = \left[1 + \left(V_e/a_j^*\right)\sin\phi\right]^{\frac{1}{2}} \tag{3}$$

where $\phi$ is the inclination of the jet thrust axis from normal to the external flow direction (measured positive into the stream) and $V_e$ is the jet exit velocity. Note that the implication of this scaling is that increase in the exit Mach number for a forward inclined thrust axis

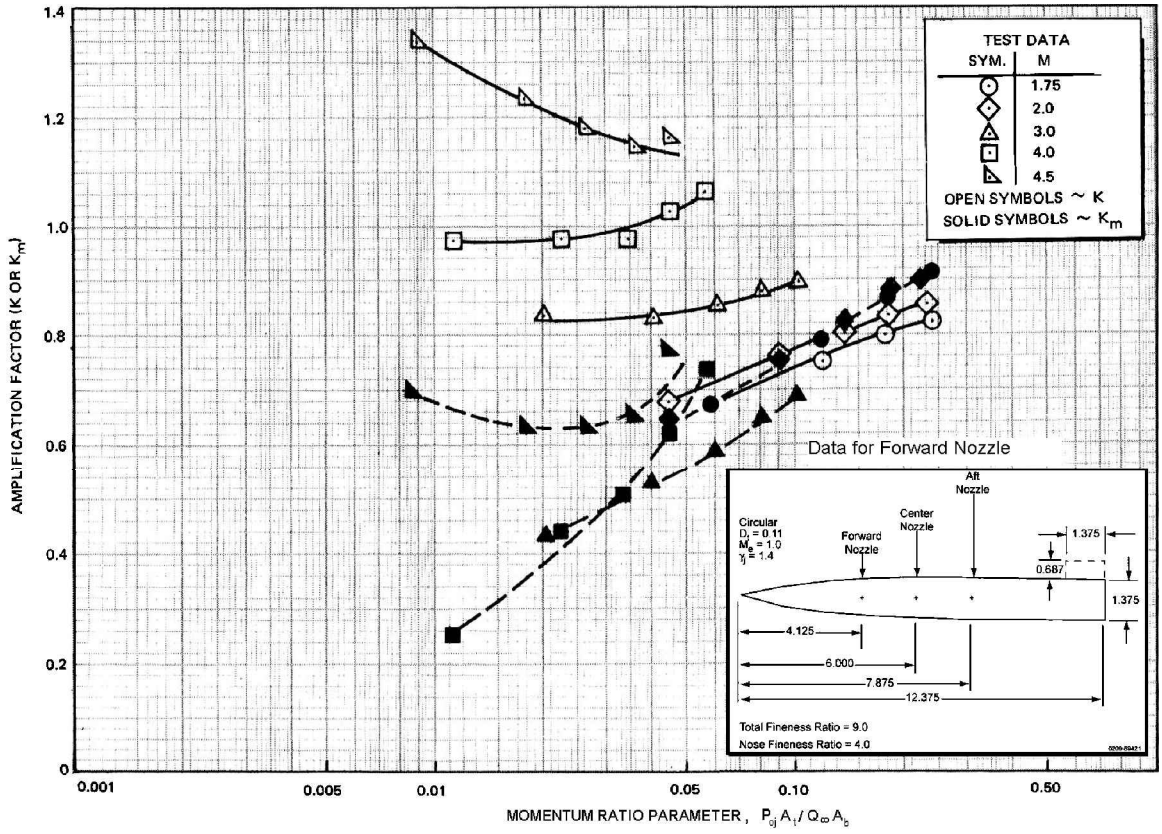


**Fig. 8 Variation in amplification factor for forward located jets.**

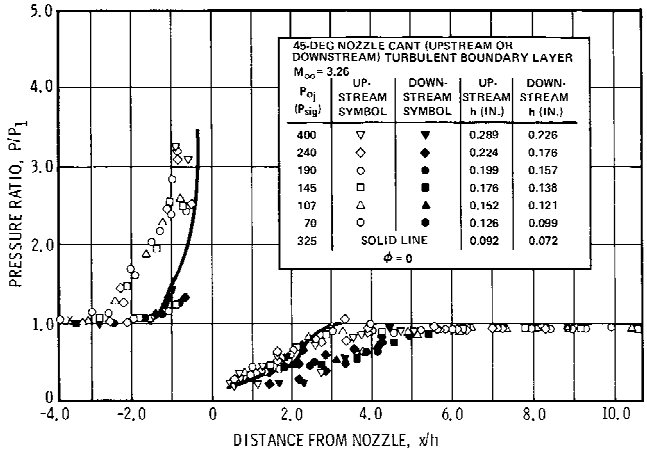


**Fig. 9 Effect of jet nozzle inclination on interaction pressures.**

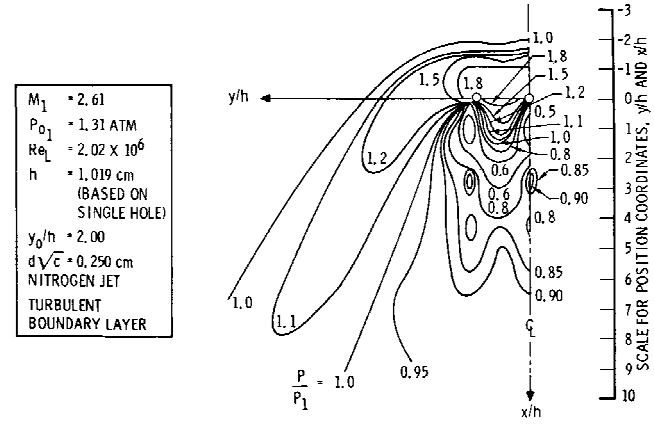


**Fig. 10 Interaction pressure contours for a pair of jet nozzles.**

increases the penetration height. Because the forward inclined jet pushes the favorable interaction region upstream, thus increasing the area of favorable interaction, increases in the jet exit Mach number would be expected to have a favorable effect. That has been observed in experiments.

The centerline pressure distributions for inclination forward and aft from normal to a uniform supersonic stream are shown in Fig. 9, from Ref. 1, based on data from Ref. 17. Also shown (by the solid line) are data for no inclination, $\phi = 0$. The effect of forward inclination driving the upstream boundary-layer separation farther forward has been observed in other experiments. The downstream inclination effect on downstream pressure distributions would not necessarily be expected to scale very well with the penetration height calculated by Eqs. (1) and (3) because the assumptions from which they were derived are based on a blockage model. They do not include the effect of entrainment and mixing at the jet boundaries.

An aspect of jet nozzle geometry that provides significant control over the aerodynamic interference is the cross-sectional shape of the nozzle, or geometry of a cluster of nozzles. As reported in Ref. 19, there is evidence that multiple circular nozzles in a line transverse to the oncoming mainstream produce an interaction that is similar to that associated with a jet from a finite-span slot, such as reported in Ref. 15. The interference pressure distribution associated with two circular jets, closely spaced transverse to the mainstream flow over a flat plate, is illustrated in Fig. 10, from Ref. 1, based on data from Ref. 19. As shown in Fig. 10, the high pressures upstream span the distance between the circular nozzles separated by eight nozzle diameters.

The effects of secondary jet thermodynamic properties, on aerodynamic interference generated by a three-dimensional jet, have been the subject of several investigations. In the perfect gas case addressed here (and in most cases in the literature involving experimental data), these effects are represented by changes in the molecular weight and stagnation temperature of the jet. Most of the early, fundamental research is reviewed in Ref. 1. Much of it dealt with the case of two-dimensional jets. The literature pertaining to jets from transverse slots is reviewed in Refs. 20 and 21. It appears that

the influences on interaction forces, in the immediate vicinity of the jet (particularly upstream of it), that are independent of changes in the jet momentum are higher order than those that correlate with jet momentum changes. It is likely this case can only be demonstrated for those situations where the principle phenomenon involved in the interaction is the blockage of the mainstream by the jet. That is the case addressed in most of the research. In the cases where the jet is on the leeside of a body at angle of attack, or near a separated flow region on a complex configuration, the blockage model may not be adequate. The mixing and entrainment process, not accurately represented by the momentum ratio models, may have more significant influence on interaction pressures. Some of these situations are addressed in Ref. 22. (See the remarks on interactions on space shuttle in Sec. III.B.)

### B. Evaluation of Unintended JI

The approach to evaluation of unintended aerodynamics interaction with reaction control plumes should begin with the selection of candidate interaction phenomena that might be associated with unintended interaction. In each case, the objective of the evaluation must be defined because it is not the result of engineering design processes. Generally, the evaluation situation results from one of two circumstances (or both). The first is a decision to employ reaction controls designed for exoatmospheric use under atmospheric flight conditions. The second is the discovery of unattributable flight dynamics anomalies that occur when reaction controls are activated, sometimes in only segments of the flight envelope (in Mach number, angle of attack, and altitude coordinates). An example of the latter is discovery of reduced control effectiveness and extraneous rolling moments on a short-range missile with stabilizer fins downstream of the jet (as in the example in Fig. 8). This example is the subject of evaluations reported in Ref. 11. There are two examples of the former that have been the subject of considerable engineering efforts reported in the literature. One is associated with the kill vehicle component of the theater high-altitude area defense (THAAD) missile defense system. Results of that evaluation are summarized in Ref. 23. Application of computational methods in that evaluation is described in Sec. IV.B. The other is associated with the space shuttle reentry configuration. The results of that evaluation have been well documented in Refs. 22 and 24, which provide an excellent, accessible history of a major engineering effort.

Late in the development of the space shuttle, the use of the reaction-control system, originally designed for onorbit operations, was adapted to the early reentry portion of atmospheric flight. There had been earlier NASA experience with unintended interaction on the X-15 research aircraft program. (In that case, unintended rolling moments were observed when reaction jets oriented to provide exoatmospheric yaw control, were activated at exo-to-endoatmospheric transition altitudes.) Consequently, an engineering analysis and ground-testing program was performed to characterize the unintended interference from the space shuttle control jets over the intended reentry flight envelope.

The geometry of the space shuttle and its reaction controls is shown in Fig. 11, reproduced from Ref. 22. Early assessments (not described in the references) of aerodynamics interference associated with operation of the forward-mounted yaw control thrusters, at high angle of attack in early reentry, indicated substantial out-of-plane rolling moments would be introduced if they were used. These appeared to be associated with the far-field vortex system, in the wake of the forward yaw control jet plume interaction (described in Sec. II), on the side of the forward fuselage. The dominant interference in that case appeared to be the effect of the vortex system streaming over the wing-lifting surface on only one side of the vehicle. A decision to rely only on the aft-located reaction controls during reentry is described in Refs. 22 and 24, as well as the analyses and testing to characterize the interference associated with these. Because these are aft-mounted thrusters, in the sense of Sec. III.A, the associated interference is dominated by phenomena in the vicinity of the plume interaction.

Unfortunately, because of the presence of the vertical stabilizer and wing lifting surfaces, the vehicle cross section is complex in

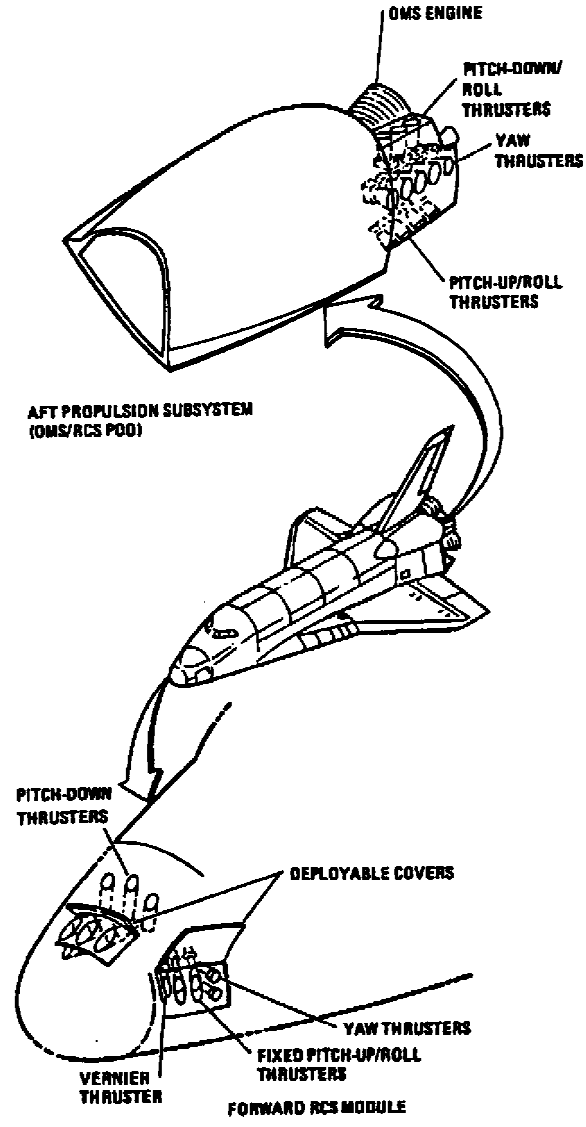


**Fig. 11 Space shuttle reaction-control configuration.**

the region of the interaction. Consequently, in the context of the remarks in Sec. III.A, the interaction forces are quite different from those that would be anticipated on a simple configuration (such as one with constant radius of curvature in the cross section near the jet). In addition, the reaction controls are only operated at very low dynamic pressure. Consequently, the scale of the plume interaction is very large, a second condition prone to unfavorable interactions.

In one set of these cases, interaction pressure disturbances from a roll control thruster were projected on the vertical stabilizer, a surface transverse to the plane of the nozzle exit. The result was a force component, transverse to the reaction force, in the vicinity of the reaction force, that is, a cross coupled yawing moment resulting from a roll control activation. In another set, the jet plume from a yaw control thruster interfered with flow separation on the leeside of the wing. The mass addition/entrainment in the separation region and plume interaction region impingement on the transverse surface changed the leeside pressure distribution on the wing. This caused a lift increment on only one wing. The result is an unintended rolling moment caused by yaw control activation.

As noted in Ref. 24, an important facet of the space shuttle aerodynamic interference evaluation was the conclusion that the scaling laws associated with the different classes of interferences appeared to be different. As noted in Ref. 24, the models and ground-test facility limitations prohibited first principles similitude of even the principal parameters of fluid mechanics scaling (to be discussed). Consequently, scaling laws were selected from the literature, and

tested against ground- and flight-test data, to determine how flight predictions should be projected from subscale ground-test data. It was observed that momentum ratio scaling seemed to fit some phenomena (principally the plume blockage/deflection of the mainstream), whereas mass flow ratio-based scaling seemed to correlate the disturbance of the lifting surface leeside flow separation configuration. The basis for expecting such differences is discussed next.

## IV. Prediction Methods

In the first two decades of applications of JI technology, there were negligible prospects for predicting aerodynamics of JI. In that era, semi-empirical methods were developed that ranged from correlations of experimentally determined force and moment data to principally inviscid flow computational models of the flowfield in the interaction region. Examples of the latter were blast wave analogies and axisymmetric flow method of characteristics solutions for solid bodies of simple geometry representing the jet plume. Most of these are summarized in Ref. 1. The most successful approaches to engineering design involved application of analytical modeling to derivation of scaling laws. Parametric wind-tunnel testing, designed around the scaling laws, determined interaction effects as a function of flight envelope parameters. Then semi-empirical fits of amplification factors provided the basis for sizing control systems. Examples of scaling law derivations are reviewed in Refs. 1 and 11. Finally, flight testing (or, for limited aspects of scaling, complex variations in wind-tunnel testing configurations) was required to validate the scaling laws, and therefore, the performance predicted. Until the results for the space shuttle were published in Refs. 22 and 24, little data were available on flight-test validation in the open literature. A bibliography of many examples that were reported with limited distribution, because of national security issues, is provided in the references in Ref. 2.

In the past two decades, a new tool has evolved. The success of computational fluid dynamics (CFD) has opened a wide range of opportunities for direct solution of virtually any level of representation of the JI flowfield under many circumstances of applications interest. Although issues related to validation of solutions exist, the prospect of combining the application of CFD with the classical tools of analytical modeling, wind-tunnel and flight testing bodes well for the engineers facing system design and flight performance evaluation problems involving JI.

### A. Design of Subscale Experiments

Approaches to derivation of similitude requirements to define models and environments for subscale simulation of JI flight conditions are discussed in Ref. 1. For the perfect gas conditions addressed here, a two-step approach is suggested. First the fundamental parameters required for similitude in the absence of the jet plume are matched. Then a set of ratios between jet and mainstream parameters is satisfied. Unfortunately, as noted in Ref. 22 with respect to the space shuttle, achievement of even simplified rigorous similitude may be impractical in available ground-testing facilities.

As an example, a common problem in achieving similitude of geometry for predicting effects on large flight vehicles is the small size of the jet nozzle that similitude requires. Because the jet is a control device, thrust levels (and, therefore, nozzle dimensions) are inherently small compared to aerodynamic lift and drag forces (determined by vehicle dimensions). Consequently, when the nozzle dimensions are scaled to the size of hypersonic wind-tunnel testing models, both tolerances (uncertainties in dimensions) and special fluid mechanics phenomena not present in the full-scale vehicle may be evoked. As an example, when the reaction control nozzle throat diameter on the space shuttle is scaled down to the approximately 1/100 scale (required for geometric similitude on a model the order of 1 ft long required for testing at 40-deg angle of attack in 3-ft test sections) a throat diameter of about 20 mil (1/200 in.) is required on the model. The Reynolds number based on that diameter is low enough that viscous effects (sometimes called discharge coefficient effects) on the nozzle flow can be significantly different than at flight vehicle scale. Conversely, mainstream total pressure must be high to generate near-flight Reynolds numbers in the mainstream of the subscale wind-tunnel model. Therefore, very high jet stagnation pressures are required to match the ratio of jet-to-mainstream total pressure. This may be impractical from structural, safety, or economics (availability) considerations

To solve this problem, a scaling parameter combining nozzle area and pressure is sought. To match such a parameter, one can be traded for the other (nozzle throat area for plenum pressure in the preceding example) in establishing similitude. Fortunately, such parameters have been derived and shown to have validity for certain aspects of the scaling problem.

#### 1. *General Similitude Requirements*

To define similitude requirements for subscale testing, the flight environment is selected as a freestream reference state, and a significant length of the vehicle, $L$, is selected as the reference length. The first requirement is geometric similitude between the external configurations of the flight vehicle and the subscale model. The parameters required for similarity in the absence of the jet plume are then

$$M_\infty = \frac{V_\infty}{\sqrt{\gamma_\infty R_\infty T_\infty}}, \qquad Re_{L,\infty} = \frac{\rho_\infty V_\infty L}{\mu_\infty}$$

$$Pr_\infty = \frac{\mu_\infty C_{P\infty}}{k_\infty}, \qquad \gamma_\infty \tag{4}$$

$$\frac{T_w}{T_\infty} = \frac{T_w}{T_\infty}\left(\frac{x}{L}, \frac{y}{L}, \frac{z}{L}\right) \tag{5}$$

Similarity can be extended to incorporate the interaction process if the geometric similitude is extended to the geometry of the jet nozzle and the following set of ratios is matched:

$$V_j/V_\infty, \qquad R_j T_j/R_\infty T_\infty, \qquad \rho_j/\rho_\infty$$

$$k_j/k_\infty, \qquad \gamma_j, \qquad \mu_j/\mu_\infty, \qquad d/L \tag{6}$$

In these parameter definitions, $d$ is a characteristic nozzle dimension and the subscript $j$ refers to a specific location within the jet flow, for instance, at the nozzle exit.

This set of simulation requirements is highly restrictive, but considerable simplification is usually warranted in scaling wind-tunnel tests. If the external flow is always air (or nitrogen), $Pr_\infty$ and $\gamma_\infty$ will be nearly matched automatically (except in some hypersonic Mach number simulations). The requirement for simulating the wall temperature distribution requires attention only when higher-order viscous interaction effects are important or when it is necessary to simulate skin friction or aeroheating precisely. Wall temperature effects are sometimes significant in determining the exact extent of the separated regions. Another problem encountered in the design of precise experiments is that simulation of the Mach and Reynolds numbers and dimensionless temperature distribution will not necessarily lead to simulation of the location of boundary-layer transition. This is partly because surface roughness effects may not be simulated, but primarily because of wind-tunnel boundary-layer noise. (In supersonic/hypersonic flight emulation, the model is seldom the same surface material as the flight vehicle.) As a result, the problem of simulating transition location is test facility unique and must usually be considered separately from other scaling requirements.

Free shear layers are nearly always turbulent at Reynolds numbers of practical interest, and so matching parameters representing transport by molecular diffusion and conduction at the shear layer boundary between the jet and the mainstream may usually be neglected. Then the only molecular transport properties that must be included are those that influence the vehicle boundary layer. In situations where the jet interaction mixing process has a significant effect, scaling parameters representative of the JI turbulent mixing process must be derived (as discussed later in connection with scaling laws). Examples are those discussed in Ref. 25.

These approximations lead to a simplified set of simulation requirements, the form of which is 1) geometric similitude with

both the body and the nozzle scaled to the same length, 2) duplication of $M_\infty$ and $Re_{L,\infty}$, and 3) duplication of $P_{0j}/P_{0\infty}$, $\gamma_j$, $(T_{0j}/M_j)/(T_{0\infty}/M_\infty)$, where $M$ is the molecular weight and the subscript 0 refers to stagnation conditions.

*2. Scaling Parameters for Interaction Phenomena*

Various idealizations of the interaction region have been proposed, from which less restrictive sets of scaling requirements then those described earlier can be derived. The general approach is to first hypothesize that an aspect of the fluid mechanics phenomena associated with the interaction can be isolated as the principle contributor in a situation of interest. Then an analytical model of that aspect of the interaction must be derived in a form that can be reduced to a parameter representing flow and geometry specifications. To be useful, these parameters must relate jet and mainstream flow conditions in such a way as to provide a degree of freedom in configuring subscale ground test or flight testing (or CFD simulation) that relieves a constraint imposed by requiring all of the described similitude parameters to be simultaneously matched.

Aspects of JI that this approach has been applied to include 1) the blockage of the mainstream by the plume, momentum exchange hypothesis and energy addition hypothesis; 2) the behavior of the vortices in the wake of the plume; and 3) mixing and entrainment at the plume/mainstream boundary.

Because their foundation is a hypothesis, the range of applicability of scaling parameters derived from each such analysis must be determined by testing them against experimental results (or as suggested subsequently by virtual testing through CFD simulation). Indeed, whether they are valid anywhere depends on the validity of the hypothesis that provided the simplifying assumptions.

An example of such an approach is the derivation of a momentum ratio scaling law. Following the analogy suggested in Ref. 15, the aspect of the flow to be addressed is the influence of the jet plume in creating an obstacle to the flow over the vehicle. The hypothesis is that the interaction pressures on the vehicle result from the mainstream flow interference caused by the obstacle. The obstacle generates a shock system in the mainstream and separates the approaching boundary layer. The hypothesis that simulation of this aspect of the flow captures the dominating phenomena governing interaction forces can be related to applications domains of pertinence. One such domain is the vehicle/jet configuration in supersonic flight where the jet exit is near the base of the flight-vehicle geometry and local separated flows are not present in the absence of the plume. Such an extended specification of the hypothesis is rigorous in excluding aspects where significant influences other than blockage may be present. In this case, that may include any phenomena associated with turbulent mixing at the jet boundaries, or the vortex system associated with it. However, validation testing may indicate deviations due to that unmodeled phenomenon that are not significant for some configurations and environments of interest.

A simplified model that represents the hypothesis is shown in Fig. 12. The jet plume is taken to be a second body attached to the vehicle. To derive a scaling law (as opposed to a method of calculating a scaling dimension), it is not necessary to specify explicitly the shape of the obstacle, as long as geometric similitude is maintained independently. The drag on the vehicle can be represented by the drag coefficient expression

$$\text{vehicle drag} = C_{Dv} q_\infty A_v \tag{7}$$

Similarly, the drag on the jet plume can be represented by defining a drag coefficient for the plume as an obstacle:

$$\text{jet plume obstacle drag} = C_{Dj} q_\infty A_j \tag{8}$$

For simplification, both drag coefficients are taken to incorporate base drag, forgiving the requirement to specify downstream conditions. The drag on the jet plume is assumed to turn the plume in the direction of mainstream flow. Then the change in momentum of the plume is

$$T(1 - \sin\theta) = C_T P_{0j} A(\cos\theta + 2\sin\theta) \tag{9}$$

where $\theta$ is the forward inclination of the thrust axis from normal to the mainstream flow and $C_T$ is the thrust coefficient. Then the ratio of jet-to-mainstream drag is

$$\frac{C_{Dj} q A_j}{C_{Dv} q A_v} = \frac{C_T P_{0j} A(1 - \sin\theta)}{C_{Dv} q A_v} \tag{10}$$

When it is presumed that the mainstream flow similitude is achieved and that the subscale model maintains geometric similitude in the direction of the thrust axis (and ignoring the effects of jet molecular weight and temperature), the parameter on the right-hand side reduces to the familiar momentum ratio scaling parameter

$$P_{0j} A^* \big/ q A_v$$

This parameter has been validated in several successful comparisons between wind-tunnel test results and flight data, such as described in Refs. 2, 22, and 24. The conclusion from those successful validations is that the dominant aspect of the interaction flow in those cases was the blockage effect of the jet plume. More important, note that there were some interference effects reported in Ref. 22 that appeared to not to correlate with the momentum ratio. As noted in Sec. III.B, these appeared to be associated with the plume interaction with a region (on the leeside of a wing art angle of attack) that already involved separated flow in the absence of the jet plume.

An analogous analysis can be applied to develop a scaling model for energy (or mass flow) ratio. In this case, the hypothesis is that interaction is dominated by deposition of energy from the jet into the mainstream flow. This hypothesis is used to derive models of scaling dimensions for the interaction region in several analyses such as Refs. 26 and 27. In principle, this model should have more general applicability. If the blockage disturbance size were scaled properly by it, it would be expected to pertain to some aspects of the cases where there is a separated flow region in the vicinity of the interaction in the absence of the jet plume. However, the hypothesis is not as direct as the momentum-scaling hypothesis in addressing the blockage phenomena for high specific momentum jet plumes.

The energy dissipated by the drag of the vehicle can be written

$$E_v = D_v V_\infty = C_{Dv} q_\infty A_v V_\infty = C_{Dv} \rho_\infty V^2 V_\infty A_V \big/ 2 \tag{11}$$

The energy added to the flow by the jet, assumed to be an adiabatic perfect gas at stagnation conditions, is

$$E_j = V\left(c_{pj} T_{0j} A^*\right) \rho_j \tag{12}$$

where $E_v$ is the mainstream energy dissipated in the vehicle drag and $E_j$ energy added to the stream by the jet. Then

$$Ej = C_{pj} T_{0j} A^* \dot{m}_j \tag{13}$$

$$E_j / E_v = 2/C_{Dv}(\dot{m}_j/\dot{m}_\infty) A^* \big/ A_v \left(C_{pj} T_{0j} \big/ V_\infty^2\right) \tag{14}$$

where

$$V_\infty^2 = a_\infty^2 M_\infty^2 = \gamma_\infty R_\infty T_\infty M_\infty^2 \tag{15}$$

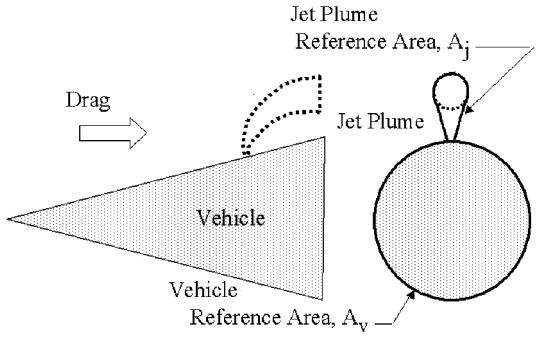


**Fig. 12 Flow model for scaling law derivation.**

After some manipulation of the perfect gas state equations, this relationship can be reduced to

$$\frac{E_j}{E_v} = \frac{2}{C_{Dv}M_\infty^2}\left(\frac{\gamma_j}{\gamma_\infty}\right)\frac{\{1+[(\gamma_\infty-1)/2]M_\infty^2\}}{(\gamma_j-1)}\left(\frac{M_\infty}{T_{0\infty}}\right)\left(\frac{T_{0j}}{M_j}\right)$$
$$\times\left(\frac{\dot m_j}{\dot m_\infty}\right)\left(\frac{A^*}{A_v}\right) = \left(\frac{1}{C_{Dv}M_\infty^2}\right)\left(\frac{\gamma_j}{\gamma_\infty}\right)\frac{\left[2+(\gamma_\infty-1)M_\infty^2\right]}{(\gamma_j-1)}$$
$$\times\frac{(T_{0j}/T_{0\infty})}{(M_j/M_\infty)}\left(\frac{\dot m_j}{\dot m_\infty}\right)\left(\frac{A^*}{A_v}\right) \tag{16}$$

In the absence of temperature and molecular weight ratio sensitivities, under subscale test conditions where similitude for the mainstream flow is achieved, the energy balance scaling reduces to mass balance scaling, that is, a requirement to match

$$\dot m_j/\dot m_\infty$$

As discussed in Ref. 1, there has been a substantial amount of experimentation leading to the conclusion that these effects are relatively unimportant in scaling interaction forces on flat plates. This is true except when the jets are inclined downstream from normal to the flow, as illustrated in Ref. 28. Independence of interaction forces upstream of the jet from changes in total temperature of the jet is reported in Refs. 20 and 21 and independence of changes in jet gas molecular weight is reported in Ref. 21. The conclusion in Ref. 24 that mass flow ratio scales the wind-tunnel results to the flight data, when the interference region includes the separated leeside of the space shuttle wing at high angle of attack seems to support extension of these conclusions. In the results reported in Ref. 24, no attempt was made to match the temperature and molecular weight ratios independently in the wind-tunnel testing that was correlated with the flight data. On the other hand, those ratios were implicitly matched in the flight data (discussed later).

In cases where the independence of scaling requirements from the temperature and molecular weight effects can be justified, the requirement to differentiate between mass and momentum ratio scaling is absent. The ratio of the two ratios is the velocity ratio:

$$\frac{\text{momentum ratio}}{\text{mass flow ratio}} = \frac{\rho_j V_j^2/\rho_\infty V_\infty^2}{\rho_j V_j/\rho_j V_\infty} = \frac{V_j}{V_\infty} \tag{17}$$

which reduces to a combination of temperature, molecular weights and Mach numbers as

$$a_j M_j/a_\infty M_\infty = M_j/M_\infty\sqrt{T_{0j}m^\infty/T_{0\infty}m_j} \tag{18}$$

Consequently, when mainstream and jet Mach exit numbers are matched, the two scaling laws are the same. Here, the results reported in Ref. 24 lead to an ambiguous conclusion with that stated earlier. That is, if the scaling was independent of temperature and molecular weight effects, why was there a difference in correlation with the two scaling laws tested against the space shuttle flight data? In the opinion of the present author, the more likely correct conclusion is that the temperature and molecular weight effects may play a role in situations such as reported in Ref. 24. There the interference forces may not be dominated by the pressure rise due to blockage effect of the jet plume. The close proximity of the separated flow region on the leeside of the wing, that is, a region where the flow is already separated in the absence of the jet plume, implies that the interaction effects on that region are likely to include mass and/or energy addition.

### B. CFD Applications

Like experiments, CFD is a powerful, but resource intensive tool, when applied to problems as complex as jet interaction. Typical solutions reported in the literature require thousands of work hours and hundreds of CPU hours of computational time. They require an infrastructure of software ranging from flow and chemistry models to geometry, solution grid, data postprocessing, and graphics capabilities. The infrastructure, personnel, and skills to maintain and apply this infrastructure, and the computational resources on which it can be exercised, are available in few circumstances. Consequently, approaches to planning their application should be similar to those employed in application of wind-tunnel and flight tests.

In the reports of successful CFD solutions, there are still issues affecting the absolute accuracy of results. Changes in fluid properties and chemistry models, viscosity models, grid structures, and time steps influence results predicted. However, the success of CFD in obtaining solutions for a wide range of models, combining different aspects of the jet interaction phenomenology, provides a powerful tool to complement wind-tunnel and flight testing. As suggested in Ref. 29, semi-empirical correlations of solutions from CFD models provide a powerful extension of the capability represented by CFD. Perhaps the most significant applications to date have been to evaluate interaction forces' sensitivity to variations in configuration and flow parameters. As the complexity of geometry and flows addressable by CFD increases, these applications become powerful design and performance anomaly analysis capabilities.

The evolution of complexity of the flowfield in CFD solutions is illustrated by the progress from two-dimensional flow solutions (for a uniform flow mainstream) in Ref. 30 to the solutions for a three-dimensional slender body at angle of attack in Ref. 31. The complexity of CFD solutions, this one for the interaction region in the vicinity of the plume, is shown in Fig. 13. Figure 13 shows temperature distributions predicted for the interaction region on an axisymmetric body at zero angle of attack. The jet is located on a flare at the base of a missile. These results were derived using the GASP code described in Ref. 32. An example of one of the more complex recent CFD models is reported in Ref. 29. The solution reported

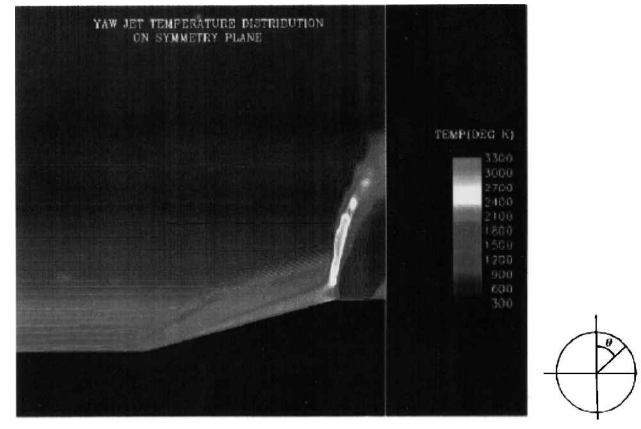


**a) Typical CFD solution for temperature isotherms in JI centerline plane**

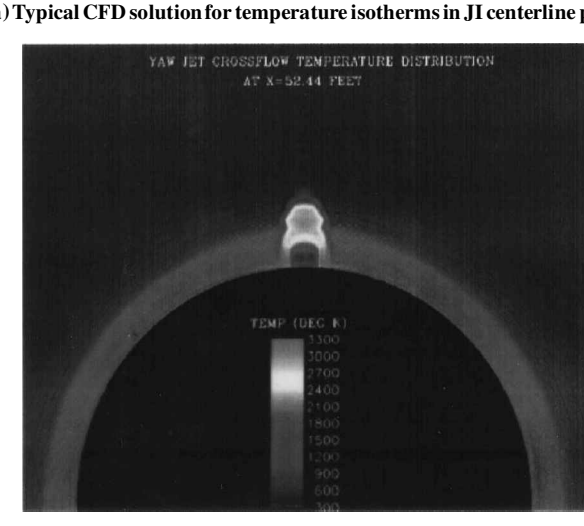


**b) Typical CFD solutions for temperature isotherms in JI cross-section plane at nozzle exit**

**Fig. 13 CFD modeling of JI.**

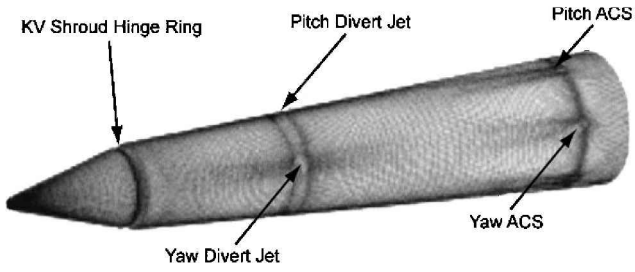


**Fig. 14 THAAD missile model.**

there is for a two-stream, axisymmetric jet in a three-dimensional flow model, with turbulent viscosity and reacting flow in the plume.

Some of the earliest successes in CFD modeling of jet interaction provided visibility into the utility of CFD as both a complement to, and as an extension of, wind-tunnel testing. An early application of CFD as an aid to experimental diagnostics of the flowfield was reported in Ref. 33. The use of CFD to evaluate the sensitivity of the flowfield solution to chemistry in the jet plume was illustrated in Refs. 34 and 35.

In Ref. 34, the influence of jet plume chemistry modeling, on interaction forces and moments, is analyzed for a large interaction plume located forward on a missile body. The simulation models a THAAD terminal stage flying at Mach 3. The configuration is illustrated in Fig. 14 reproduced from Ref. 34. The thruster modeled is termed a divert thruster. It is large enough to provide lift (or vehicle translation) forces and located near the center of the length (at the c.g.) of the biconic configuration. Flight altitude and associated freestream conditions are the independent variables. Even though the vehicle geometry downstream of the jet exit is a conical surface (no fins or lifting surfaces present), and the condition modeled is zero angle of attack, the interaction induced forces and moments are substantial. Simulations of the interaction are reported for two altitude conditions, 15 and 30 km. Even at the lower altitude, the thrust is large enough that the interaction region penetrates the body shock layer more than a body diameter at the jet location and continues to grow downstream (as indicated by species concentrations predicted). At the higher altitude, the jet plume is not turned by the mainstream flow, until after it has passed through the bow shock of the vehicle. The results of the study are summarized in Fig. 15 reproduced from Ref. 34.

The results of four simulation models are shown in Fig. 15 reproduced from Ref. 34. The first (labeled air) is a model of the most common wind-tunnel testing approach, where both the jet plume and the mainstream are the same perfect gas. The second model (labeled binary) treats the two as different perfect gases, in this case by changing the ratio of specific heats in the jet plume from that used in the first case. The other two models treat the plume as the products of combustion of a monomethyl-hydrazine/nitrous oxide propellant ($MMH/N_2O_4$) reaction. In one of these real gas cases (labeled Frozen), the reaction products are frozen at the jet exit. In the other case (labeled Reacting), reaction rates (and the resulting state changes along the interacting flow downstream of the jet plume) are modeled. The ordinate in Fig. 15 is the increment in JI-induced pitching moment, from a longitudinal increment of interaction-induced pressure, normalized by a constant reference moment. Positive increments are associated with positive pressure in the plane of the jet exit. The abscissa is dimensional length along the missile. As discussed in Sec. III.A.1, the location of the jet nozzle in the midsection of the body leads to interaction moments that generally oppose the direction of the jet thrust. That is clearly the case for all conditions represented here. The difference in moment distributions between the two altitude conditions, shown in Figs. 15a and 15b, indicates that the interaction moment decreases with increasing altitude, or increasing size of the interaction disturbance, a trend associated with this geometry and scale of interaction.

The significant difference in effects predicted by the different models is indicated in Fig. 15. Two effects of jet plume chemistry are predicted. The first is the influence, on the interaction pressure distribution, of the change in plume thermodynamic properties. This

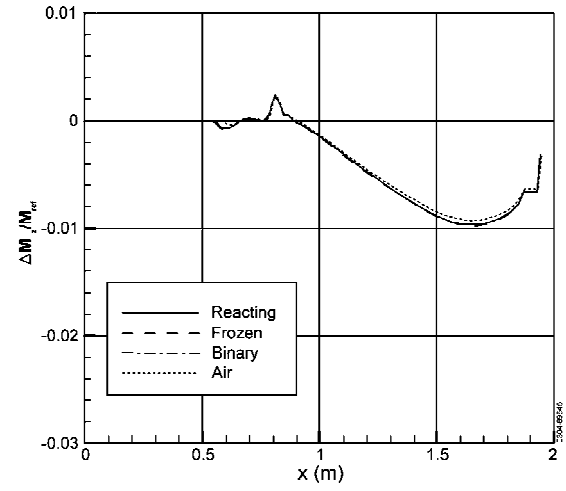


**a) 30-km-altitude simulation**

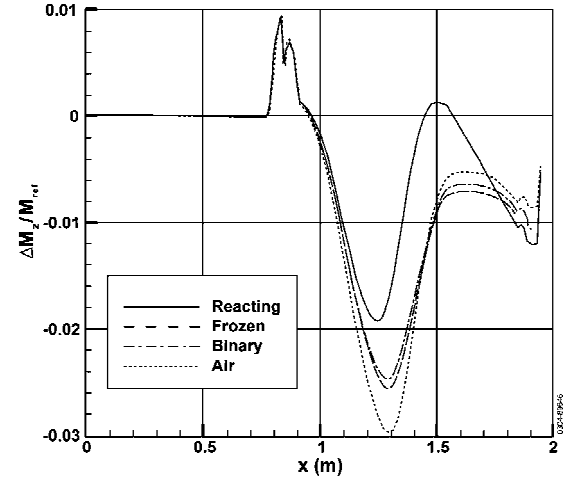


**b) 15-km-altitude simulation**

**Fig. 15 Effect of plume chemistry model on CFD predictions of JI-induced moments.**

is illustrated by the difference between the case labeled Air and the cases labeled Binary and Frozen, which represent similar, constant thermodynamic properties that are different from those of air (principally ratio of specific heats). As demonstrated in Ref. 34, the moment difference predicted by the simulation is principally the effect of diminishing the low pressures, on the body downstream of the jet exit, in the wake of the jet plume. The second, and even more dramatic, effect predicted is the influence of interaction flowfield-dependent chemistry on the interaction. Continuing finite rate chemical reactions (termed afterburning), in the jet plume downstream of the jet exit, cause an increase in pressure on the missile surface (compared to the cases where there is no continuing chemistry change downstream). Analysis results described in Ref. 34 indicate that the continuing reactions are exothermic and that they depend on oxygen from the mainstream interacting with the plume. The description of vortex-induced mixing in this region in Sec. II.B suggests why increased levels of mainstream oxygen may be entrained into the plume.

As noted in Ref. 34, it is not clear that a scaling model (such as those suggested in Sec. IV.A.2) could be derived to design subscale simulations of the this phenomena, if they are limited to nonreacting gases in the mainstream and jet. As noted in Sec. IV.A.2, models based on energy balance postulates are more likely to scale interactions dominated by mixing between the plume and mainstream flows than momentum balance-based models. Such models may compensate for the effects in the interaction due to changes in thermodynamic properties in the plume (Binary and Frozen models, compared to Air in Fig. 15). However, they are unlikely to

compensate for continuing exothermic reactions when those effects are large.

Several reported applications of CFD illustrate its use in determining the location of the jet as a reaction-control device. As discussed in Sec. III.A, favorable interactions, that is, interference-induced forces in the direction of jet thrust, are usually associated with jet locations on the vehicle afterbody. However, in many applications, either design constraints (such as packaging interference with propulsion systems or separable lower stages) or performance objectives (such as use of the reaction control as a side force generator in high-altitude conditions) dictate jet locations forward on the vehicle. The effects of the low pressures in the wake of the plume and wraparound of the interaction bow shock on the interaction pressure in the immediate vicinity of the jet were reported in Ref. 36. In this case, the vehicle configuration is a body of revolution. The jet location on the body could be moved to more aft positions, preserving the body-alone and forward flowfield solutions with efficiency in resources required. A similar, but more complex (more recent and more successful) solution, with four jet nozzle plumes from rectangular cross section nozzles was reported in Ref. 37. These two studies represent evolution of a Navier–Stokes equation solver CFD system referred to as the PARC code. In the latter study, the downstream system of vortices in the wake of the jet interaction is resolved in conjunction with the set of vortices in the leeside separation region of the vehicle at angle of attack. Thus, the effect of jet location on downstream interactions could have been evaluated if jet location were varied.

Complete interaction flowfield CFD solutions for a slender missile at angle of attack, with a jet located forward on the missile and fins located on the afterbody, were reported in Ref. 38.

The extension of these CFD applications to include the evaluation of the influence of body geometry in the vicinity of the jet is reported in Refs. 31 and 39. In Ref. 39, the effects of jet thrust inclination into the mainstream (forward relative to the body centerline on a slender body of revolution) are evaluated for a jet located forward on the body. The increase in unfavorable interactions downstream of the jet are found to dominate the increase in favorable interactions forward of the jet. As discussed in Sec. III.A, vehicle cross section in the vicinity of the jet can significantly influence the unfavorable effects of the interaction bow shock wrapping around the vehicle downstream of the jet exit. In Ref. 31, strakes, in the plane perpendicular to the jet thrust, close to the jet exit form a concave reflection plane for the bow shock. CFD solutions of Navier–Stokes equations illustrate the favorable effect of moving the strakes to the vicinity of the jet nozzle. The vehicle is a slender body of revolution. The unfavorable interference effect of moving the strakes aft, to a different geometry of intersection with the interaction bow shock is illustrated. These solutions resolve the vortices in the wake of the interaction and their effect on stabilizer or control surfaces far downstream of the plume. Further evidence that the three-dimensional effects downstream of the jet produce the unfavorable interaction is supported by the two-dimensional (slot spanning a flat plate) solution described in Ref. 30. There, the forward inclination of the thrust produced favorable interaction.

### C. Combining CFD, Wind-Tunnel, and Flight Testing

The success of CFD applications reviewed provides an additional powerful tool to the applications engineer designing to incorporate or evaluate the effects of jet interaction. References to successful CFD solutions discuss the issues associated with the art of CFD applications and the uncertainties of flow properties modeling. There are invariably discrepancies between some measurements and the CFD results. These issues should not detract from the use of the CFD capability to evaluate influences of changes in geometry and flow properties on interaction effects in aerodynamics engineering (at least not at the current state of the art in evaluating jet interaction aerodynamics). In fact, as indicated in Ref. 31, many jet interaction aerodynamics effects can be determined sufficiently accurately for some applications with inviscid flow models. Some further CFD experimentation, such as reported there, could lead to very efficient applications of such models. The key to efficient application of the CFD tool is to integrate it with the derivation of scaling rules through analytical modeling, the use of semi-empirical representations in parametric analyses, and wind-tunnel and flight testing. Such an approach is suggested in Ref. 29.

Compared to wind-tunnel testing, CFD has the advantage that separation of variables, in parametric evaluations, is more easily accomplished. In wind-tunnel testing, there are invariably facility, instrumentation, model fabrication, and acceptability of operating gases constraints on variations in parameters. Consequently, changing variables independently in a scaling parameter and repeating solutions (presuming a successful solution exists for a particular vehicle/jet configuration and flight environment) should be an efficient application of CFD. An example would be to change stagnation pressure and throat area independently, at a constant value of the momentum scaling parameter derived in Sec. IV.A.2 and to evaluate the effect on interaction-induced forces and moments (or jet throat area and vehicle base area could be changed independently). After a scaling parameter is validated, its range of applicability could be tested by varying environments over the intended flight envelope. Where there is divergence from a particular scaling law, other alternatives can fairly readily be tested, for example, changing molecular weight and stagnation temperature of the jet gas independently, or their relationship to those properties in the mainstream, to test an energy release scaling parameter.

With scaling parameters associated with applicable segments of the intended flight envelope validated, the interaction forces and moments can be predicted as functions of the scaling parameters and environment variables, for example, angle of attack, Mach number, and altitude. Then semi-empirical fits, such as defined in Refs. 2 and 22 for an experimental database, can be developed (based on the CFD-generated database) for use in vehicle and control system design and sizing. Once a baseline vehicle and reaction-control system configuration is designed through this application of approximations, CFD can again be applied to confirm/perturb performance predictions for critical points in the flight envelope. Because CFD can be applied to wind tunnel as well as flight conditions and scales, comparison between the CFD and design verification wind-tunnel testing can be used to evaluate the uncertainty in the CFD predicted results.

The successful application of CFD to chemically reacting jet plumes, such as reported in Refs. 34 and 40 (summarized earlier), to explore the significance of chemical reactions in fuel-rich jets, represents a powerful capability. Scaling of rate-dependent reacting flows with subscale geometry, in ground (or flight) tests, is at least as problematic as the uncertainties in CFD solutions. CFD sensitivity studies that vary parameters, such as presence and absence of chemistry, can provide valuable insight into the applicability of scaling laws without demonstrating that the calculations agree exactly with what is measured in experiment (though, in many cases, they may).

Whether or not chemical reactions in the flow are addressed, the availability of successful CFD modeling provides a valuable tool for planning and augmenting the function of flight testing in validating interaction scaling laws. In most cases of practical interest in supersonic (and certainly in hypersonic) flight applications, full-scale ground testing to validate prediction of interaction effects is not a viable alternative (as it was not in the space shuttle case reported in Refs. 22 and 24 and flight tests described in Ref. 2). In fact, rigorous similitude is seldom an alternative and was not in those cases. Consequently, to bridge from the wind tunnel (or other propulsion ground test) to flight when CFD models are viable, the question is how best to use them. Clearly, CFD is not constrained by the problems of dimensional scale associated with wind-tunnel testing. In addition, CFD offers the ability to combine Mach number, altitude, and angle of attack, with dimensional scale beyond similitude possible in the wind tunnel (and, in the case of hypersonic flight vehicles, unachievable without wide trajectory variability and/or risks in experimental flight test). Historically, certainly for hypersonic flight conditions in turbulent boundary-layer environments, the only recourse for validation of scaling parameters including dimensional similitude was comparison between measurements from ground and flight testing. With CFD, the first-order validation only requires a

repeat of a successful solution with the dimensions and state parameters changed. Obviously, many of the other variables usually associated with the difference between wind tunnel and flight testing such as chemical reactions, gas properties, or surface boundary conditions can also be varied. Certainly, the accuracy of CFD modeling becomes more uncertain as it is extended to incorporate solutions to equations with less certain validity of pertinence than the Navier–Stokes equations for continuum flow. However, those with experience in trying to perform these validations, constructing similitude between wind tunnel and flight testing, appreciate the immense difficulty usually associated with trying to vary parameters such as these independently in flight tests. Therefore, because some of these difficulties (and some different ones, such as turbulence and heat transfer modeling) will always be encountered with CFD should not impede prudent progress in application of such a powerful capability. Even when flight testing is used as a tool to analyze phenomenology as complex as JI, the difficulty associated with the collection and interpretation of measurements leaves uncertainties in accuracy. Application of CFD in parametric analyses and planning should reduce the burden on measurements required in flight testing for validation and calibration. It should certainly make the span of the envelope validated larger and the confidence in the validation higher.

## V. Conclusions

The state of the art in understanding JI phenomenology has long been sufficiently advanced to provide guidance for the aerodynamics engineer in analysis or design applications. Scaling laws for design of wind-tunnel tests and extrapolation of data have been derived and validated. Care for the principals of similitude, and the postulates on which the models are based, must be exercised in their application. Analyses of results from flight have shown domains of applicability as well as regions where specific scaling does not (and perhaps should not be expected to) apply. Many of the references in Ref. 2 are indicative that substantial validation (or at least approaches to it) have been accomplished but have not been in the open literature. In any case, as with the data from space shuttle flights referred to earlier, flight-test validation results (or the results from any experiment or simulation) may be very specific-configuration oriented. Consequently, they require careful interpretation in application to a problem remote from the configuration and conditions of the experiment.

Notably absent in the open literature is any characterization of the aeroheating associated with JI phenomenology in supersonic or hypersonic flight. Its absence from the literature on successful CFD applications is not encouraging, but may be associated with the lack of experimental data to validate them.

The current state of the art in application of CFD to the evaluation JI problems appears to be in rapid expansion. The next step should be to combine that effort with use of CFD in support of flight-test validation of scaling parameters. Through this combination, scaling laws can be validated and used to interpolate and extrapolate the results from parametric CFD solutions. These same validated scaling laws can then be used to design wind tunnel and flight experiments for final validation of absolute values of aerodynamics characterizing system performance over the flight envelope.

## References

[1]Spaid, F. W., and Cassel, L. A., "Aerodynamic Interference Induced by Reaction Controls," AGARDograph AGARD-AG-173, NATO, Dec. 1973.

[2]Roger, R. P., "The Aerodynamics of Jet Thruster Control for Supersonic/Hypersonic Endo-Interceptors: Lessons Learned," AIAA Paper 99-0804, Jan. 1999.

[3]Mitchell, J. W., "An Analytical Study of a Two-Dimensional Flow Field Associated with Sonic Secondary Injection into a Supersonic Stream," Vidya Corp., 9166-TN-2, Mountainview, CA, March 1964.

[4]Romeo, D. J., and Sterrett, J. R., "Aerodynamic Interaction Effects ahead of a Sonic Jet Exhausting Perpendicularly from a Flat Plate into a Mach Number 6 Free Stream," NASA TN-D-743, April 1961.

[5]Spaid, F. W., and Zukoski, E. E., "Study of the Interaction of Gaseous Jets from Transverse Slots with Supersonic External Flows," *AIAA Journal*, Vol. 6, No. 2, 1968, pp. 205–212.

[6]Kistler, A. L., "Fluctuating Wall Pressure Under a Separated Supersonic Flow," *Journal of the Acoutical Society of America*, Vol. 36, No. 3, 1964, pp. 543–550.

[7]Speaker, W. V., and Ailman, C. M., "Spectra a;-id Space–Time Correlations of the Fluctuating Pressures at a Wall Beneath a Supersonic Turbulent Boundary Layer Perturbated by Steps and Shock Waves," Douglas Aircraft Co., Rept. SM-49806, Santa Monica, CA, Nov. 1965.

[8]Barnes, J. W., Davis, J. G., and Tang, H. H., "Control Effectiveness of Transverse Jets Interacting with a High-Speed Free Stream," Vol. 1, *Design Charts, Theoretical and Experimental Results*, U.S. Air Force Flight Dynamics Lab., AFFDL-TR-67-90, Wright–Patterson AFB, OH, July 1967.

[9]Romeo, D. J., "Aerodynamic Interaction Effects Ahead of Rectangular Sonic Jets Exhausting Perpendicularly from a Flat Plate into a Mach Number 6 Free Stream," NASA, TN-D-1800, May 1963.

[10]Street, T. A., "An Oil Flow Study of a Sonic Reaction Jet Ejecting from a Body of Revolution into a Free Stream of Mach Number Range 1. 75 to 4. 5," U.S. Army Missile Command, Rept. RD-TR-70-7, Redstone Arsenal, AL, April 1970.

[11]Cassel, L. A., Davis, J. G., and Engh, D. P., "Lateral Jet Control Effectiveness Prediction for Axisymmetric Missile Configurations," U.S. Army Missile Command, Rept. RD-TR-68-5, Redstone Arsenal, AL, June 1968.

[12]Durando, N. A., and Cassel, L. A., "Viscous Effects in the Interaction Flowfield Near a Jet in a Subsonic Crossflow," U.S. Army Missile Command, Rept. RD-TR-70-31, Redstone Arsenal, AL, Dec. 1970.

[13]Reid, C. F., "The Effect of Several Forward Monted Control Jet Nozzles on a Typical Missile Configuration at Transonic Speeds," Cornell Aeronautical Lab., Inc., Rept. AA-2267-W-3, Buffalo, NY, July 1967.

[14]Spaid, F. W., Zukoski, E. E., and Rosen, R., "A Study of Secondary Injection of Gases into a Supersonic Flow," Jet Propulsion Lab., TR-32-834, California Inst. of Technology, Pasadena, CA, Aug. 1966.

[15]Zukoski, E. E., and Spaid, F. W., "Secondary Injection of Gases into a Supersonic Flow," *AIAA Journal*, Vol. 2, No. 10, 1964, pp. 1689–1696.

[16]Dahlke, C. W., "An Experimental Investigation of Downstream Flowfield Properties Behind a Forward Located Jet Injected Into a Transonic Freestream from a Body of Revolution," U.S. Army Missile Command, Rept. TD-TM-68-2, Redstone Arsenal, AL, Jan. 1968.

[17]Street, D. R., "Effects of Injection Nozzle Configuration on Secondary Injection into Supersonic Flow," Mechanical Engineer Thesis, California Inst. of Technology, Pasadena, CA, 1966.

[18]Koch, L. N., and Collins, D. J., "The Effect of Varying Secondary Mach Number and Injection Angle on Secondary Gaseous Injection into a Supersonic Flow," AIAA Paper 70-552, May 1970.

[19]Spaid, F. W., Zukoski, E. E., and Rosen, R., "A Study of Secondary Injection of Gases into a Supersonic Flow," Jet Propulsion Lab., Rept. TR-32-834, California Inst. of Technology, Pasadena, CL, Aug. 1966.

[20]Chrans, L. J., and Collins, D. J., "Stagnation Temperature and Molecular Weight Effects in Jet Interaction," *AIAA Journal*, Vol. 8, No. 2, 1970, pp. 287–293.

[21]Chambers, R. A., and Collins, D. J., "Stagnation Temperature and Molecular Weight Effects in Jet Interaction," *AIAA Journal*, Vol. 8, No. 3, 1970, pp. 584, 585.

[22]Rausch, J. R., and Roberts, B. B., "Reaction Control System Aerodynamic Interaction Effects on the Space Shuttle Orbiter," *Journal of Spacecraft and Rockets*, Vol. 12, No. 11, 1975, pp. 600–666.

[23]Chamberlain, R., and McClure, D., "CFD Analysis of Lateral Jet Interaction Phenomena for the THAAD Interceptor," AIAA Paper 2000-0963, Jan. 2000.

[24]Kanipe, D. B., "Plume/Flowfield Jet Interaction Effects on the Space Shuttle Orbiter During Entry," *Journal of Spacecraft and Rockets*, Vol. 20, No. 4, 1983, pp. 351–355.

[25]Jacobsen, L. S., Gallimore, S. D., Schetz, J. A., and Brian, W. F., "An Improved Aerodynamic Ramp Injector in Supersonic Flow," AIAA Paper 2001-0519, Jan. 2001.

[26]Broadwell, J. E., "Analysis of the Fluid Mechanics of Secondary Injection for Thrust Vector Control," *AIAA Journal*, Vol. 1, No. 5, 1963, pp. 1057–1075.

[27]Dahm, T. J., "The Development of an Analogy to Blast-Wave Theory for the Prediction of Interaction Forces Associated with Gaseous Secondary Injection into a Supersonic Stream," Vidya Div., TN 9166-TN-3, Itek Corp., Mountainview, CA, May 1964.

[28]Tomioka, S., Jacobsen, L. S., and Schetz, J. A., "Angled Injection Through Diamond-Shaped Orifices into a Supersonic Stream," AIAA Paper 2001-1762, April 2001.

[29]Praharaj, S. C., Roger, R. P., Chan, S. C., and Brooks, W. B., "CFD Computations to Scale Jet Interaction Effects from Tunnel to Flight," AIAA Paper 97-0406, Jan. 1997.

[30]Clark, S. W., and Chan, S. C., "Numerical Investigation of a Transverse Jet for Supersonic Aerodynamic Control," AIAA Paper 92-0639, Jan. 1992.

[31]Srivastava, B., "Lateral Jet Control of a Supersonic Missile: CFD Predictions and Comparison to Force and Moment Measurements," AIAA Paper 97-0639, Jan. 1997.

[32]"The General Aerodynamic Simulation Program," GASP User's Manual, Ver. 3, Aerosoft, Inc., Blacksburg, VA, May 1996.

[33]Shang, J. S., McMaster, D. L., Scaggs, N., and Buck, M., "Interaction of Jet in Hypersonic Cross Stream," *AIAA Journal*, Vol. 27, No. 3, 1989, pp. 323–329.

[34]Chamberlain, R., Dang, A., and McClure, D., "Effect of Exhaust Chemistry on Reaction Jet Control" AIAA Paper 99-0806, Jan. 1999.

[35]Warfield, M. J., "Calculation of Supersonic Interacting Jet Flows," AIAA Paper 89-0666, Jan. 1989.

[36]Yeneriz, M. A., Davis, J. C., Cooper, G. K., and Harvey, D. W., "Comparison of Calculation and Experiment for a Lateral Jet from a Hypersonic Biconic Vehicle," AIAA Paper 89-2548, July 1989.

[37]Roger, R. P., and Chan, S. C., "CFD Study of the Flowfield Due to a Supersonic Jet Exiting Into a Hypersonic Stream from a Conical Surface: II," AIAA Paper 93-2926, July 1993.

[38]Chan, S. C., Roger, R. P., Edwards, G. L., and Brooks, W. B., "Integrated Jet Interaction CFD Predictions and Comparison to Force and Moment Measurements for a Thruster Attitude Controlled Missile," AIAA Paper 93-3522, Aug. 1993.

[39]Srivastava, B., "CFD Analysis and Validation of Lateral Jet Control of a Missile," AIAA Paper 96-0288, Jan. 1996.

[40]Kennedy, K., Walker, B., and Mikkelsen, C., "Jet Interaction Effects on a Missile with Aerodynamic Control Surfaces," AIAA Paper 99-0807, Jan. 1999.

T. Lin
*Associate Editor*